Journal of Colloid and Interface Science **235,** 391–397 (2001)
doi:10.1006/jcis.2000.7318, available online at http://www.idealibrary.com on IDEAL®

Force Measurements between Semifluorinated Thiolate Self-Assembled Monolayers: Long-Range Hydrophobic Interactions and Surface Charge

T. Ederth,*,[1] K. Tamada,† P. M. Claesson,* R. Valiokas,‡ R. Colorado, Jr.,§ M. Graupe,§ O. E. Shmakova,§ and T. R. Lee§

*Department of Chemistry, Surface Chemistry, Royal Institute of Technology, SE-100 44 Stockholm, Sweden, and Institute for Surface Chemistry, Box 5607, SE-114 86 Stockholm, Sweden; †National Institute of Materials and Chemical Research (NIMC), Tsukuba, Ibaraki 305-8565, Japan; ‡Department of Physics and Measurement Technology, Linköping University, SE-581 83 Linköping, Sweden; and §Department of Chemistry, University of Houston, Houston, TX 77204-5641

Received August 11, 2000; accepted October 30, 2000

Long-range interactions between self-assembled monolayers (SAMs) of semifluorinated alkanethiols have been studied by direct force measurements in water and aqueous NaCl solutions. SAMs prepared from three different thiols, with identical fluorinated head groups but varying hydrocarbon spacer lengths, were investigated: $CF_3(CF_2)_9(CH_2)_xSH$, where $x = 2$, 11, or 17. Force measurements show that the interactions in water and electrolyte solutions are composed of both double-layer interactions emerging from what appears to be charges adsorbed onto the surfaces and long-range "hydrophobic" attractions, in excess of the expected van der Waals forces. The three investigated thiols produce similar results in force measurements, though the contact angles with water are slightly different. The "hydrophobic" attraction has the form of step-like attractive discontinuities in the force profiles at separations ranging from 20 to 40 nm, caused by bridging of microscopic bubbles residing at the surfaces. The shape or range of these discontinuities are not significantly affected by replacement of the water with either 1 mM or 1 M NaCl solutions. The origin of the charges causing the electrostatic double-layer interaction is unclear, but some possible causes are discussed.

Key Words: **self-assembled monolayers; flourocarbons; interfacial charge; surface forces; hydrophobic interaction; ion adsorption.**

1. INTRODUCTION

The use of self-assembled organic monolayers (SAMs) to modify the surface or interfacial properties of materials such as noble metals, silicon, quartz, and metal oxides is a well-established method that has been a subject of intensive research over the last two decades (1, 2). In particular, the adsorption of thiols onto gold is a valuable tool for increasing the understanding of interfacial properties, as well as a method with many exploited or potential technological applications in biomaterials science, microelectronics, corrosion protection, microcontact printing, heterogeneous catalysis, and chemical sensors, to mention but a few (3). The major advatanges of this surface modification method are that it produces stable and well-defined films, and it provides a possibility to vary the surface or interfacial properties within wide limits; by functionalization of the adsorbed species, or by mixing different species, the wetting properties, the surface charge, or the density of a particular functional group on the surface can be altered. Fluorinated thiolate SAMs are of interest in this respect because of their very low surface energy and wettability.

The film structure of semifluorinated thiol or disulfide SAMs has been studied extensively (4–14). In particular, the molecular packing of $CF_3(CF_2)_7(CH_2)_2SH$ on Au(111) has been determined by various surface characterization techniques (4–8, 13), and it has been established that the helical fluorocarbon tails form densely packed layers with a hexagonal lattice (nearest-neighbor distance ≈5.8 Å). In these SAMs, fluorocarbon chains are expected to be aligned nearly normal to the surface. On the other hand, with longer alkyl spacer groups ($CF_3(CF_2)_9(CH_2)_xSH$, $x = 6$, 11, 17, 33) (7, 12–14) the helix is more tilted relative to the surface normal due to the interaction between alkyl spacer groups, resulting in different wetting properties and thermal stability for these SAMs (13).

We here report a study where the interfacial properties of SAMs formed from semifluorinated alkanethiols have been studied in water and aqueous electrolyte solutions using direct force measurements. The findings are of relevance to the study of the long-range "hydrophobic" interaction, and to the problem of the origin of the interfacial charge at oil/water interfaces.

2. EXPERIMENTAL

Three different semifluorinated thiols were investigated, $CF_3(CF_2)_9(CH_2)_xSH$, where $x = 2$, 11, or 17, which will be referred to as $F_{10}H_x$.

The semifluorinated thiols were synthesized using methods described in a previous report (15), and analytical data for the compounds will be published separately (16, 17). For reference, measurements with hexadecanethiol (Fluka, >95%) were also made. The thiolate SAMs were prepared by adsorption onto thin gold films on supports in the shape of either spheres (for surface

[1] To whom correspondence should be addressed. Present address: Physical and Theoretical Chemistry Laboratory, South Parks Road, Oxford OX1 3QZ, UK. Fax: +44 (0)1865 275410. E-mail: ederth@physchem.ox.ac.uk.

0021-9797/01 $35.00

force measurements) or plates (20×12.5 mm^2 glass slides with 0.15-mm thickness for contact angle and atomic force microscopy studies and 20×40 mm^2 Si wafers with native oxide for infrared reflection–absorption measurements). To prepare the spheres, borosilicate glass rods with 2-mm diameter were melted in one end using a butane–oxygen burner, this procedure yields spherical surfaces with RMS roughness of 0.1 nm (18). The substrates were mounted in an ultrahigh vacuum electron-beam evaporation system (Balzers UMS500P), where a 1-nm Ti adhesion layer was deposited, followed by a 10-nm Au layer (the glass plates used in contact angle measurements were coated on both sides). Thicknesses were monitored using a quartz thickness monitor with 0.1-nm resolution. Evaporation pressures were typically less than 3×10^{-8} Torr. The substrates were immersed in the thiol solutions immediately after removal from the vacuum chamber. Thiols were absorbed from 1 mM solutions in CH_2Cl_2 (or ethanol, in the case of hexadecanethiol) for at least 15 h before use. Samples were used up to 2 weeks after preparation, and no differences in results were observed for surfaces used after overnight adsorption and those used after 2 weeks. Contact angle measurements were performed using the Wilhelmy plate method (Krüss 12 Tensiometer system), at an immersion rate of 2 mm/min.

Atomic force microscope (AFM) images of the SAM surfaces were acquired with a NanoScope IIIa (Digital Instruments, Inc., Santa Barbara, CA) with Si_3N_4 cantilevers (spring constant 0.38 N/m, scanning rate 20–30 Hz). All images (512×512 pixels) were collected in the height mode (11).

A Bruker IFS66 system, equipped with a grazing angle (85°) reflection accessory and a liquid nitrogen cooled MCT detector was utilized for Fourier-transform infrared reflection–absorption spectroscopy (FTIR-RAS) measurements. The spectrometer was continuously purged with dry nitrogen gas during the measurements. The acquisition time was around 10 min, the resolution was at 2 cm^{-1}, and a three-term Blackmann–Harris apodization function was applied to the interferograms before Fourier transformation. In order to eliminate the interference effects due to the ultrathin gold substrates, the FTIR-RAS spectra of $F_{10}H_2$ and $F_{10}H_{17}$ were smoothed using OPUS (Bruker) software.

The surface force measurements were made with a bimorph surface force instrument (19). The instrument measures the force between two surfaces of arbitrary shape and material, as long as they are smooth and rigid enough to make data interpretation possible. One surface is mounted on a piezoelectric bimorph deflection sensor (20), while the other surface is moved through a two-stage positioning system; a motorized translation stage is used for rough positioning and a piezoelectric tube actuator for acquisition of force–distance profiles. The expansion of the latter is monitored with a displacement transducer, the output of which is used to compensate for the nonlinear expansion of the piezotube and to determine the sensitivity of the measuring spring (when the surfaces are brought into contact, the movement of one surface is directly translated to the spring-mounted surface). The distance resolution was of the order of 0.2 nm, and the normalized force resolution (F/R) was approximately 10 μN/m. Data are presented as forces normalized with the harmonic mean of the radii of the surfaces, F/R, where $R = R_1R_2/(R_1 + R_2)$.

3. RESULTS AND DISCUSSION

3.1. SAM Structure

The structure of the semifluorinated thiol SAMs on the 10-nm Au/glass substrates was characterized with AFM and FTIR-RAS and compared with that on Au(111)/mica surfaces (11–13). We could obtain regular lattice images on $F_{10}H_2$ (Fig. 1) and (with increasing difficulty) $F_{10}H_{11}$ SAMs, while these were not possible to obtain on the $F_{10}H_{17}$ SAMs, due to the increased disorder in the layer as the length of the methylene spacer increases (14). Unlike similar SAMs on Au(111), the lattice constant showed some scatter, presumably due to the roughness of the gold surface; see Fig. 2. However, even though regular lattices were not always observed, it was confirmed that the semifluorinated thiols form densely packed SAMs even on these thin gold layers, in a manner similar to that on Au(111) (14).

The FTIR-RAS analysis confirms the presence of $F_{10}H_2$ and $F_{10}H_{17}$ SAMs. In the CH_2 stretch region (not shown), very weak peaks are possible to identify for $F_{10}H_2$, and for $F_{10}H_{17}$ the asymmetric and symmetric stretches are around 2920 and 2851 cm^{-1}, respectively. In the fingerprint region, Fig. 3, the two typical groups of the specific bands resulting from perfluorocarbon chains can be found (4, 7, 8, 13). First, the two peaks around 1376 and 1347 cm^{-1} are assigned to axial progression CF_2 stretching modes, originating from the helical structure of the fluorocarbon chains. Second, the region between 1300 and 1100 cm^{-1} consists of overlapping bands due to the modes having their transition dipole moment perpendicular to the helical axis, asymmetric and symmetric CF_2 stretching, CC stretching, and CCC bending. The peak around 1079 cm^{-1} in $F_{10}H_2$ is probably a CC gauche mode (13), while 1263 cm^{-1} is unassigned.

Somewhat higher intensities for the axial modes and lower intensities for the perpendicular modes are observed in the $F_{10}H_2$ spectrum compared to the corresponding bands in the $F_{10}H_{17}$ spectrum. This suggests a perpendicular alignment of the fluorocarbon helixes relative to the surface for the first compound, while this alignment is less pronounced for the second (13). To summarize, the FTIR-RAS spectra of the SAMs on the ultrathin gold films are almost identical to those on more common substrates (13), revealing the striking resemblance between the structures of the SAMs.

3.2. Contact Angle Measurements

Results from contact angle measurements are summarized in Table 1, where contact angles for hydrocarbon SAMs are also included for comparison.

All samples exhibit slightly higher contact angles compared with flat Au(111) (13), which can be understood as an influence

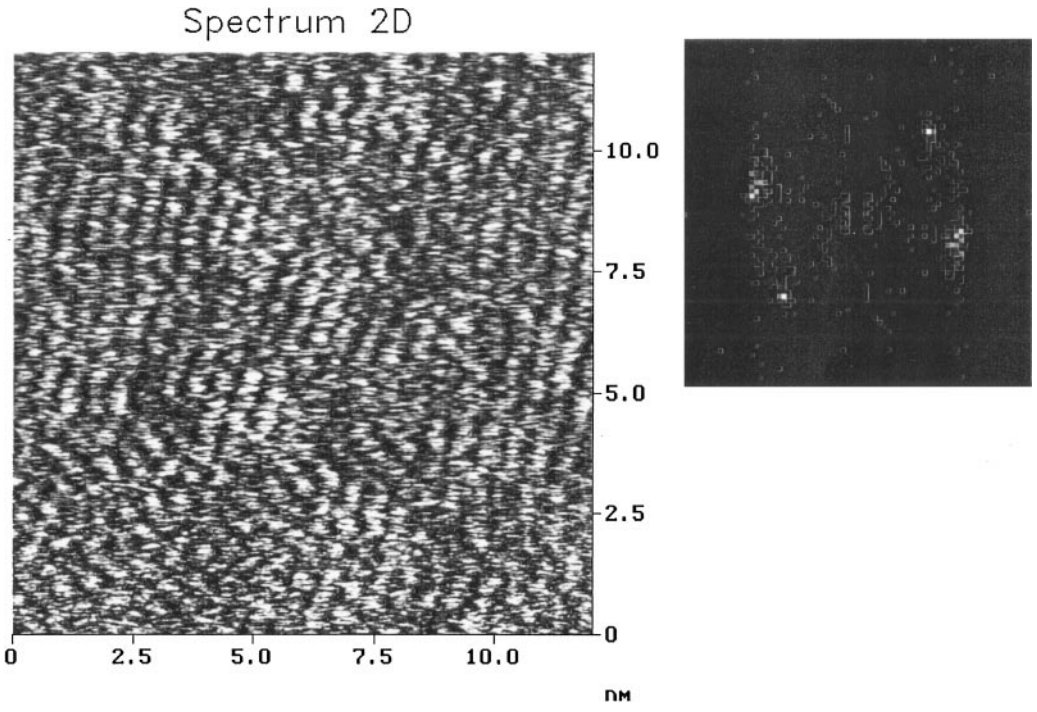

FIG. 1. AFM image of $F_{10}H_2$ on a polycrystalline gold surface and the 2-dimensional Fourier transform of the image. Increasing hydrocarbon spacer length makes reproduction of regular lattices difficult; this was never possible with $F_{10}H_{17}$ thiols, and only occasionally possible with $F_{10}H_{11}$.

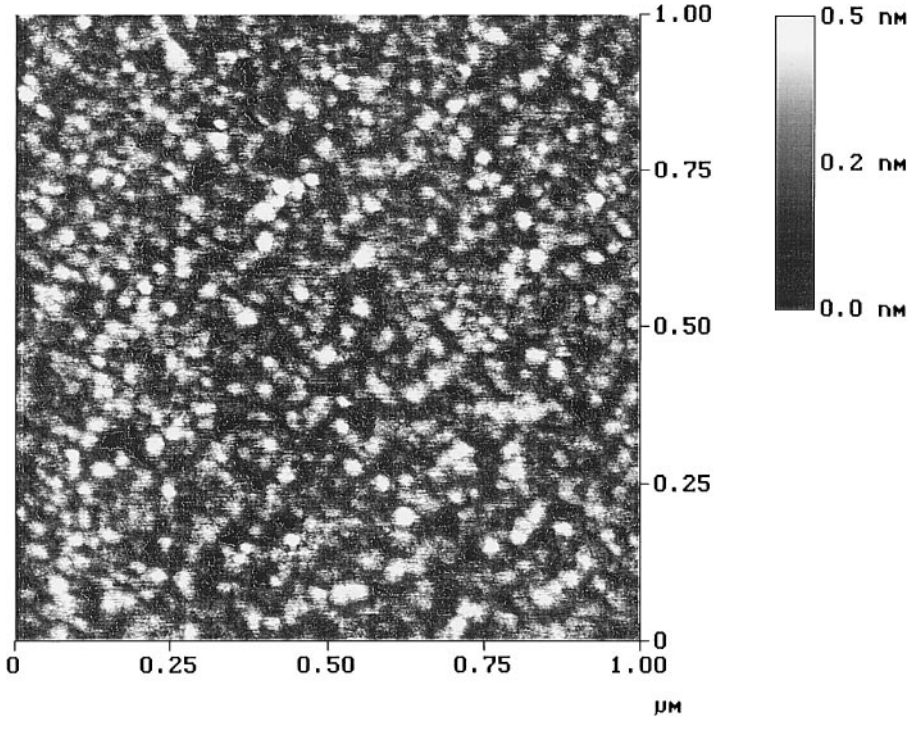

FIG. 2. AFM image of the polycrystalline gold substrate, revealing the granularity of the 10-nm gold layer, deposited onto a glass or silica surface.

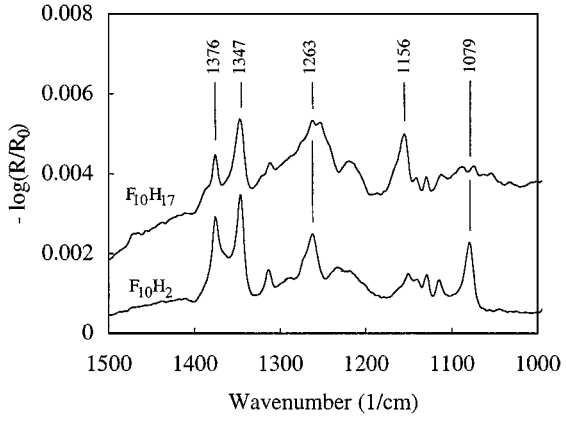

FIG. 3. FTIR-RAS spectra of $F_{10}H_2$ and $F_{10}H_{17}$. The two bands at 1347 and 1376 cm^{-1} are axial progression CF_2 stretch modes, while those between 1300 and 1100 cm^{-1} are mainly overlapping symmetric and asymmetric CF_2 stretching, CC stretching, and CCC bending modes (see text for details).

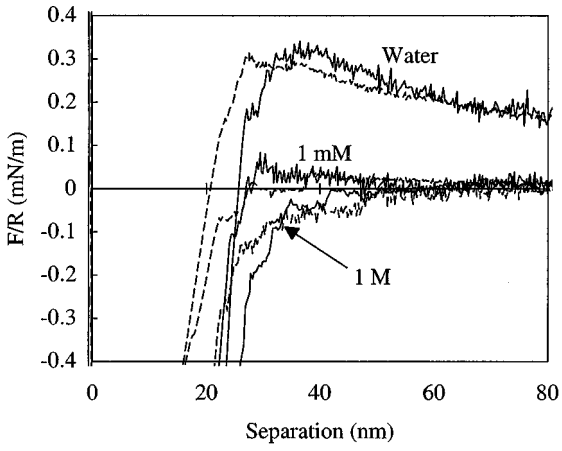

FIG. 4. Interactions between $F_{10}H_2$ (solid lines) and $F_{10}H_{17}$ (dashed lines) thiolate surfaces in water, 1 mM NaCl, and 1 M NaCl. Results from the different thiolates are indistinguishable; the different slopes at short separations (in the spring instability region, where the surfaces jump together) reflect the differences in spring stiffness in the two experiments. The repulsion is purely electrostatic, caused by what appears to be negative charges on the surfaces.

of greater surface roughness (21). The slightly lower contact angle for $F_{10}H_2$ as compared to the other semifluorinated surfaces is attributed to differences in the van der Waals interactions between the underlying gold layer and the contacting liquid, as discussed in Refs. (13, 22). It is interesting that $F_{10}H_{11}$ exhibits rather large hysteresis compared with the other SAMs, while it showed the smallest hysteresis on flat Au(111) surfaces (13). There is no obvious reason for this discrepancy; the $F_{10}H_{11}$ samples were perhaps contaminated, but it might be an effect of the different substrate as well. For the semifluorinated compounds, the ideal film structure is affected by the lengths and interactions between both the spacers and the head groups, as well as by the geometry of the lattice of adsorption sites on the gold surface. Different spacer lengths thus result in different film structures. If, for the $F_{10}H_{11}$, small changes in this balance cause the overall packing of the spacers to be inferior to what is obtained on Au(111) substrates, the mobility of the adsorbed molecules might be increased, and the contact angle hysteresis enhanced. However, for this to be true, it is required that the orientational mobility of adsorbed $F_{10}H_{11}$ be higher than it is for $F_{10}H_2$ and $F_{10}H_{17}$ on the same substrates. The former is probably true, considering the lower degree of order as observed in AFM images, though the latter seems unlikely.

3.3. Surface Force Measurements

The behavior of the three different semifluorinated compounds in force measurements appears to be similar; thus the data presented for one of the species can be taken as representative also of the other two. Data from $F_{10}H_2$ and $F_{10}H_{17}$ thiolates are compared in Fig. 4 for measurements in water and 1 mM and 1 M NaCl. Results for $F_{10}H_{11}$ are similar (no data shown). The differences between the data sets are comparable to the variations within the data for each type of surface. For a particular pair of surfaces, the apparent surface charge is constant for each electrolyte concentration, while the separation where the onset of the attraction occurs varies randomly in the range 20 to 40 nm, even for consecutive approaches. The used measurement procedure did not permit the very first approach at a particular point of contact to be recorded.

In water and aqueous electrolyte solutions, the partly fluorinated surfaces exhibit behavior that is consistent with the presence of negative charges, and the interaction is dominated by an electrostatic double-layer interaction at separations exceeding 40 nm, while at shorter separations, a strong attraction with step-like force onset is dominating. Adding electrolyte to the system does not significantly change the attractive part of the interaction, while the magnitudes and ranges of the electrostatic repulsion are diminished in accordance with DLVO theory. Data for water, 1 mM NaCl, and 1 M NaCl are compared in Figs. 4 and 5. The thick solid lines in Fig. 5 represent DLVO theory (assuming constant surface charge conditions), resulting in a surface potential of −75 mV, and a decay length of 800 Å for the data in pure water. The corresponding area per surface charge (as calculated using the Grahame equation) is 180 nm^2. The surface potentials thus obtained in water were scattered over the range −65 to −80 mV, with most of the data between −70 and −75 mV. This spread is caused by difficulties in fitting DLVO theory to water data, due to the very long decay length of the interaction, and by variations in the electrolyte concentration in "pure" water. The variations are made evident by comparing the results for

TABLE 1
Contact Angles with Water (±2°)

	θ_a	θ_r	$\Delta \cos\theta$
$CF_3(CF_2)_9(CH_2)_2SH$	120	109	0.17
$CF_3(CF_2)_9(CH_2)_{11}SH$	124	104	0.32
$CF_3(CF_2)_9(CH_2)_{17}SH$	124	114	0.15
$CF_3(CH_2)_{15}SH$	110	104	0.10

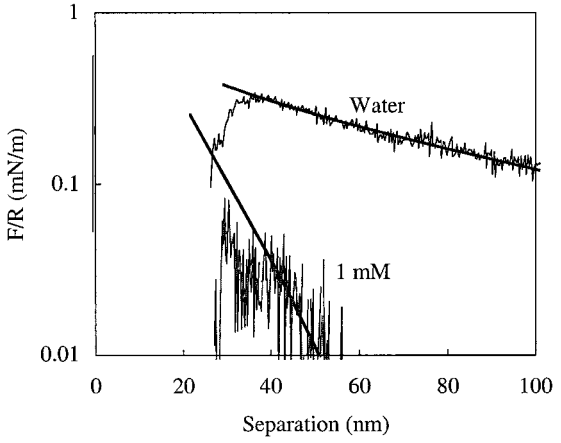

FIG. 5. Parts of the data in Fig. 4, on a semilog scale. The DLVO-fits indicated by the solid lines were made in the region outside the first onset of the attraction (approximately at 40 nm in both curves), resulting in the following figures. For water: $\psi = -75$ mV, $\kappa^{-1} = 800$ Å, area per charge 180 nm^2. For 1 mM NaCl: $\psi = -60$ mV, $\kappa^{-1} = 96$ Å, area per charge 30 nm^2.

water in Fig. 4 with those in Fig. 6, where a different set of data is shown.

As small amounts of electrolyte are added, the spread in the data is reduced, even though the separation range over which the fitting can be performed is much smaller. For 1 mM NaCl, the potential is typically −60 mV, and the corresponding area per charge is approximately 30 nm^2. At 1 M NaCl, the very short decay length of the electrostatic contribution (3 Å) effectively removes the electrostatic repulsion from the measurable range of interactions. The only effect of adding electrolyte to the solution is to reduce the decay length of the repulsion, while the attraction remains unchanged. We thus conclude that whatever the mechanism behind the attraction is, it is not affected by the presence of electrolyte.

The attraction is of the same character as that observed between hydrocarbon thiolate surfaces, see Fig. 6. Several publications discuss such step-like attractive onsets between hydrophobic surfaces in terms of bridging of bubbles attached to the surfaces, and the attraction at shorter separations as the result of the spreading of the formed capillary (18, 23–25), and for thiolated gold surfaces with particular reference to the imperfections at the surfaces caused by the polycrystallinity of the gold substrate (26). These provide plenty of nucleation sites for bubbles or cavities where air could be trapped. This is likely to be the explanation for the observed behavior also in this case: the surfaces are hydrophobic and the absorbates are rigidly attached, the underlying gold structure is similar, and the formation of bubbles is anticipated also on these surfaces. Recent experiments show that the formation of these bubbles is dependent on exposure of the surfaces to air before measurement (25, 27), indicating that these bubbles are trapped during immersion of the surfaces in water rather than nucleated at the surfaces. Apparently, the fact that the surfaces are charged does not interfere with the attraction, i.e., the formation of a water vapor or gas capillary and the subsequent spreading over the two surfaces during its growth. Also included in Fig. 6 is a force profile for a pair of hydroxylated thiolate surfaces interacting in water (data taken from Ref. (18)), whose van der Waals interaction is expected to be similar to the interaction between the hydrophobic hydrocarbon surfaces, and not significantly different from the van der Waals contribution for the fluorinated surfaces (the measured curve agrees with a van der Waals force calculated using a Hamaker constant of approximately 4×10^{-20} J).

To determine the sign of the surface charge, one of the fluorinated surfaces was replaced by a flame-polished bare glass surface (prepared as described above), which is known to have a negative surface charge. The electrostatic interactions in these asymmetrical systems were always repulsive (Fig. 7), indicating that the charge of the fluorinated surfaces is also negative

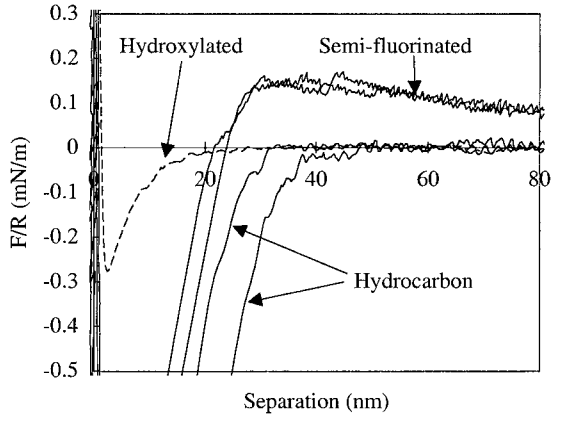

FIG. 6. Results for semifluorinated surfaces compared with data for hydrocarbon surfaces. The data for hydroxylated surfaces (dashed line), which are expected to interact only through van der Waals interaction, are taken from Ref. (18). All force profiles were obtained in pure water.

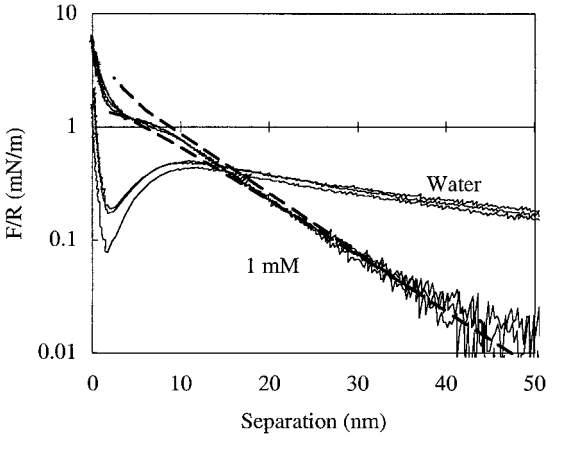

FIG. 7. Interactions between a semifluorinated thiolate surface and a bare glass surface, in pure water and in 1 mM NaCl. Since the glass surface is negatively charged, the repulsive electrostatic force is evidence that also the fluorinated surface is negatively charged. The dashed lines correspond to Poisson–Boltzmann fits to the data for 1 mM under constant charge (upper) and constant potential (lower) conditions; with the surface potential for the semifluorinated surface fixed at −60 mV, the resulting potential for the glass surface is −50 mV.

in water. Fitting the data for the interaction in 1 mM NaCl to the Poisson–Boltzmann model resulted in a surface potential of approximately −50 mV for the glass surface, if the potential of the semifluorinated surface was fixed at −60 mV. The absence of a distinct attractive van der Waals interaction in 1 mM NaCl is probably caused by repulsive steric interaction with a gel-like silica layer on the glass surface (28) (note that the thick dashed lines in Fig. 7 represent Poisson–Boltzmann, not DLVO theory). Such a gel would swell in electrolyte, as compared to its state in water, thus explaining the differences in the apparent van der Waals forces in water and 1 mM NaCl in Fig. 7. We note that in previous force measurements in asymmetrical systems consisting of a mica surface and a hydrophobic Langmuir–Blodgett film, an additional long-range attraction was observed, in excess of the DLVO prediction, and of the same character as the attraction between two hydrophobic surfaces (29). Further, in a study using mica surfaces made hydrophobic by surfactant adsorption, the interaction between a hydrophobic surface with a hydrophilic mica surface was of similar qualitative behavior, but stronger than the interactions between two hydrophobic surfaces (30). The fact that no unexpectedly long-range attraction is observed between the glass surface and the fluorinated surface confirms that the "hydrophobic" forces observed between fluorinated (and hydrocarbon) thiolate surfaces have a different origin than those observed between surfaces made hydrophobic by LB-deposition or surfactant adsorption, as has been described recently (31).

The electrostatic repulsion observed between the semifluorinated surfaces is not present in the interactions between hydrocarbon surfaces; force measurements in water between hexadecanethiol surfaces do not indicate the presence of surface charge, while the same discontinuous attractive force onsets are present; see Fig. 6. The fact that no electrostatic repulsion is observed between the hydrocarbon surfaces does not imply that the surfaces are not charged, but rather that an upper limit to the charge can be estimated. Assuming that the electrolyte concentration in pure water is 1×10^{-5} M, the detection of electrostatic repulsive forces at separations $\geq$40 nm would be difficult (with the resolution of our instrument) if the magnitude of the surface potential is $\lesssim$15 mV. The possible presence of charge at the thiolate hydrocarbon/water interface has been touched upon by Kokkoli *et al*., who claim that the surface potential is $\leq$1.7 mV (32), but this conclusion seems not to be supported by their data. The normalized accuracy of their AFM was $\pm$0.016 nN/10 μm = 0.0016 mN/m, and they state that "no attractions were measured up to the point where the probe jumped into contact." At a jump separation of 5 nm, the attractive van der Waals force, using a Hamaker constant for hexadecane (which is their expected lower limit for the magnitude of the attraction), is 0.033 mN/m. This is $>20\times$ the claimed accuracy, but still no attraction was measured; thus we find the claimed upper limit of the surface charge doubtful, as well.

The charging of purportedly neutral surfaces in water was observed at the beginning of the 20th century, when air bubbles in water were observed to carry negative charge in electrokinetic experiments (33, 34), and this was later also observed in thin-film drainage experiments (35). The charging of oil/water interfaces is a similarly well-known phenomenon which has been known for almost as long, but it is still a matter of research (36, 37). It is not surprising to find that the ions naturally occuring in water have different affinities to a particular surface, but as yet we are not in a position to explain the difference in surface charge of the fluorinated surfaces, as compared to the hydrocarbon surfaces. The approach of an ion in water toward a surface of lower dielectric constant is an electrostatically unfavorable process, and more so the lower the dielectric constant of the other medium (38). In view of this, the charging of the fluorocarbon–water interface appears to be less favorable than the charging of the hydrocarbon–water interface, suggesting that it is the result of some specific ion–surface interaction, which is not present at the hydrocarbon surface, or due to some property particular to perfluorinated alkanethiols.

Marinova *et al*. measured the electrophoretic mobility of both hydrocarbon and fluorocarbon oil droplets in water, and found the ζ-potentials of both hydrocarbon and perfluorinated oils to be in the range −50 to −60 mV (37). It was suggested that the charge at the water/oil interface originates from an asymmetry in the hydrogen-bond network at a hydrophobic surface that favors the presence of OH^- ions at the interface. The differences between this result and the data reported here suggest that, as regards the electrostatic properties of the surface, it is of relevance that in the thiolated surfaces the molecules form a solid layer with all molecules aligned in an ordered structure. Although a regular lattice was not observed on the surfaces with the longest hydrocarbon spacer, the molecules at least are aligned, while not being ideally close-packed. It is uncertain to what extent the comparison with liquid oil droplets is relevant, but on the face of it, the results by Marinova *et al*. seem to suggest that perhaps it is the uncharged hydrocarbon surfaces that behave anomalously, rather than the perfluorinated; then again, if the proposed mechanism cannot account for the differences we observe, it might not be appropriate in either case.

The observed differences in apparent surface charge are in qualitative agreement with a surface potential study of alkanethiol monolayers: Evans *et al*. observed that the surface potential of (hydrocarbon) alkanethiols is positive, while a monolayer where the upper part is perfluorinated results in a large negative value (39). This difference was suggested to be due to the high electronegativity of the fluorine atoms. Experiments where perfluorinated silanes are used to modify glass or silica surfaces often indicate the presence of surface charge, though the variations in electrostatic properties of surfaces modified with the same silanes point to the underlying glass, and inconsistent silanization, as the source of the charge, rather than the perfluorinated surface itself (compare Refs. (40, 23) for an example). We do not have any evidence as to what the charging mechanism for the perfluorinated surfaces is, but we here consider some alternatives. First, an obvious source is contamination, though the

similarity of the electrostatic properties of all tested substrates makes this less likely. It is possible that the charging of the semifluorinated surface is the result of van der Waals interaction between ions and the surface (41). This could be the situation if the differences in polarizability between hydrogen and fluorine atoms are large enough to make the latter attract ions in the solution through dispersion interaction. Also, the attachment of a fluorocarbon segment to a hydrocarbon chain generates a strong dipole (42, 43), which might attract hydroxyl ions in the water through induction-type interactions. Further, the oriented dipoles in the $-CF_2-CH_2-$ junctions form a dipole layer that might contribute to the interaction. Carlton and Winkle proposed that the intermolecular electrostatic repulsion between perfluoroalkanes is greater than that between corresponding alkanes, since the surface atoms of the former molecules are the negative ends of highly polar bonds (44), and although this interaction cannot be the cause of the observed repulsion, it is perhaps possible that this effect is related to the charging of the perfluorinated surfaces in water. Thinking along new lines entirely, we note that fluorocarbon compounds have the capacity to dissolve large amounts of gases (so well, in fact, that they are considered as artificial blood substitutes (45, 46)), and if this is true also for the fluorocarbon segments in these films, it is conceivable that, e.g., dissolved CO_2 ionizes at the interface. It might be of some importance that the fluorocarbon segments are not close-packed in the same way as plain hydrocarbons are in SAMs, but have a helix structure (47) whose diameter is approximately 5.5–6 Å.

ACKNOWLEDGMENTS

We thank Professor B. Liedberg, Linköping University, for generous permission to use the surface preparation facilities in his laboratory, Dr. H. Fukushima, Seiko Epson Co., for valuable discussions, Dr. J. Fröberg for assistance with fitting in asymmetrical electrolytes, and the Swedish Natural Science Research Council (NFR) for financial support. The work at the University of Houston was supported by the National Science Foundation (DMR-9700662) and by Seiko Epson Corporation.

REFERENCES

1. Ulman, A., "An Introduction to Ultrathin Organic Films." Academic Press, Boston, 1991.
2. Dubois, L. H., Nuzzo, R. G., *Annu. Rev. Phys. Chem*. **43,** 437 (1992).
3. Xu, J., and Li, H.-L., *J. Colloid Interface Sci*. **176,** 138 (1995).
4. Alves, C. A., and Porter, M. D., *Langmuir* **9,** 3507 (1993).
5. Chidsey, C. E. D., and Loiacono, D. N., *Langmuir* **6,** 682 (1990).
6. Lui, G. Y., Fenter, P., Chidsey, C. E. D., Ogletree, D. F., Eisenberger, P., and Salmeron, M., *J. Chem. Phys*. **101,** 4301 (1994).
7. Tsao, M.-W., Hoffmann, C. L., Rabolt, J. F., Johnson, H. E., Castner, D. G., Erdelen, C., and Ringsdorf, H., *Langmuir* **13,** 4317 (1997).
8. Lenk, T. J., Hallmark, V. M., Hoffman, C. F., Rabolt, J. F., Castner, D. G., Erdelen, C., and Ringsdorf, L., *Langmuir* **10,** 4610 (1994).
9. Schönherr, H., and Vansco, G. J., *Langmuir* **13,** 3769 (1997).
10. Schönherr, H., and Ringsdorf, H., *Langmuir* **12,** 3891 (1996).
11. Schönherr, H., Ringsdorf, H., Jaschke, M., Butt, H.-J., Bamberg, E., Allison, H., and Evans, S. D., *Langmuir* **12,** 3898 (1996).
12. Tamada, K., Nagsawa, J., Nakanishi, F., Abe, K., Hara, M., Knoll, W., Ishida, T., Fukushima, H., Miyashita, S., Usui, T., Koini, T., and Lee, T. R., *Thin Solid Films* **327–329,** 150 (1998).
13. Fukushima, H., Seki, S., Nishikawa, T., Takiguchi, H., Tamada, K., Abe, K., Colorado R., Jr., Graupe, M., Shmakova, O. E., and Lee, T. R., *J. Phys. Chem. B* **104,** 7417 (2000).
14. Tamada, K., Ishida, T., Fukushima, H., Knoll, W., Colorado, R., Jr., Graupe, M., Shmakova, O. E., and Lee, T. R., in preparation.
15. Graupe, M., Koini, T., Wang, V. Y., Nassif, G. M., Colorado, R., Jr., Villazana, R. J., Miura Y. F., Shmakova, O. E., and Lee, T. R., *J. Fluorine Chem.* **93,** 107 (1999).
16. Colorado, R., Jr., Shmakova, O. E., Graupe, M., and Lee, T. R., in preparation.
17. Frey, S., Heister, H., Zharnikov, M., Grunze, M., Tamada, K., Colorado, R., Jr., Graupe, M., Shmakova, S., and Lee, T. R., *Isr. J. Chem.*, in press.
18. Ederth, T., Claesson, P., and Liedberg, B., *Langmuir* **14,** 4782 (1998).
19. Parker, J. L., *Prog. Surf. Sci*. **47,** 205 (1994).
20. Stewart, A. M., *Meas. Sci. Technol*. **6,** 144 (1995).
21. Abe, K., Takiguchi, H., and Tamada, K., *Langmuir* **16,** 2394 (2000).
22. Miller, W. J., and Abbott, N. L., *Langmuir* **13,** 7106 (1997).
23. Parker, J. L., Claesson, P. M., and Attard, P., *J. Phys. Chem.* **98,** 8468 (1994).
24. Carambassis, A., Jonker, L. C., Attard, P., and Rutland, M. W., *Phys. Rev. Lett.* **80,** 5357 (1998).
25. Boehnke, U.-C., Remmler, T., Motschmann, H., Wurlitzer, S., Hauwede, J., and Fischer, T. M., *J. Colloid Interface Sci*. **211,** 243 (1999).
26. Ederth, T., and Liedberg, B., *Langmuir* **16,** 2177 (2000).
27. Ishida, N., Sakamoto, M., Miyahara, M., and Higashitani, K., *Langmuir* **16,** 5681 (2000).
28. Vigil, G., Xu, Z., Steinberg, S., and Israelachvili, J., *J. Colloid Interface Sci*. **165,** 367 (1994).
29. Claesson, P. M., Herder, P. C., Blom, C. E., and Ninham, B. W., *J. Colloid Interface Sci*. **118,** 68 (1987).
30. Tsao, Y. H., Evans, D. F., and Wennerström, H., *Langmuir* **9,** 779 (1993).
31. Christenson, H. K., and Claesson, P. M., *Adv. Colloid Interface Sci.*, in press.
32. Kokkoli, E., and Zukoski, C. F., *Langmuir* **14,** 1189 (1998).
33. Alty, T., *Proc. R. Soc. London A* **106,** 315 (1924).
34. McTaggart, H. A., *Philos. Mag.* **27,** 297 (1914).
35. Mysels, K. J., and Jones, M. N., *Disc. Faraday Soc.* **42,** 42 (1966).
36. Dickinson, W., *Trans. Faraday Soc.* **37,** 140 (1941).
37. Marinova, K. G., Alargova, R. G., Denkov, N. D., Velev, O. D., Petsev, D. N., Ivanov, I. B., and Borwankar, R. P., *Langmuir* **12,** 2045 (1996).
38. Israelachvili, J. N., "Intermolecular and Surface Forces," 2nd ed. Academic Press, London, 1985.
39. Evans, S. D., and Ulman, A., *Chem. Phys. Lett.* **170,** 462 (1990).
40. Parker, J. L., and Claesson, P. M., *Langmuir* **10,** 635 (1994).
41. Ninham, B. W., Kurihara, K., and Vinogradova, O. I., *Colloids Surf. A* **123–124,** 7 (1997).
42. Shafrin, E. G., and Zisman, W. A., *J. Phys. Chem.* **61,** 1046 (1957).
43. Graupe, M., Takenaga, M., Koini, T., Colorado, R., Jr., and Lee, T. R., *J. Am. Chem. Soc.* **121,** 3222 (1999).
44. Carlton, T. S., and Winkle, R. J., *J. Fluorine Chem.* **65,** 1 (1993).
45. Maugh, T. H., *Science* **179,** 669 (1973).
46. Frietsch, T., Lenz, C., and Waschke, K. F., *Eur. J. Anaesthesiol.* **15,** 571 (1998).
47. Bunn, C. W., and Howells, E. R., *Nature* **174,** 549 (1954).